Uptake and Retention Kinetics of *Para*-Fluorine-18-Fluorobenzylguanidine in Isolated Rat Heart

Clifford R. Berry, Pradeep K. Garg, Michael R. Zalutsky, R. Edward Coleman and Timothy R. DeGrado
Department of Anatomy, Physiological Sciences and Radiology, North Carolina State University, College of Veterinary Medicine, Raleigh; and Department of Radiology, Duke University Medical Center, Durham, North Carolina

Para-[^{18}F]fluorobenzylguanidine ([^{18}F]PFBG) is a newly developed tracer for imaging myocardial sympathetic neuronal innervation. This study investigated the uptake and retention mechanisms of [^{18}F]PFBG in perfused, isolated rat heart. **Methods:** Fluorine-18-PFBG was administered to working rat hearts within the perfusion medium at a constant activity concentration (1.5–2 MBq/liter) for 8 min, followed by a washout period (50 min). External scintillation probes with coincidence detection circuitry were used to measure myocardial radioactivity. Six groups of hearts (n = 6, except in Group 6) were studied: (Group 1) control; (Group 2) 100 n*M* desipramine (DMI); (Group 3) 0.8 μ*M* SKF550; (Group 4) DMI + SKF550; (Group 5) SKF550 + 1.0 μ*M* Ro 4-1284; and (Group 6) SKF550 with DMI chase at 30 min (n = 4). **Results:** Groups 2, 3 and 4 showed a mean reduction of 19% (uptake-1 blockade), 58% (uptake-2 blockade) and 95% (uptake-1 and uptake-2 blockade) in uptake rates, respectively, compared with control ($p < 0.01$). A further 33% reduction in the uptake rate was noted with vesicular transport inhibition (Group 5 compared with 3, $p = 0.054$). Biphasic clearance consisting of rapid ($T_{1/2} = 5.32 \pm 1.1$ min) and slow ($T_{1/2} = 35.2 \pm 9.6$ min) components were noted in control hearts. The rapid ($T_{1/2} = 1.6 \pm 0.3$ min) and slow ($T_{1/2} = 10.9 \pm 1.4$ min) clearance rates were accelerated ($p < 0.0001$) in Group 5 compared to control. DMI chase conditions (Group 6) caused an inhibition of [^{18}F]PFBG washout ($p = 0.004$) suggesting a role for reverse transport through the uptake-1 carrier. **Conclusion:** Fluorine-18-PFBG is specifically accumulated by sympathetic nerve terminals. However, further work is recommended in humans to evaluate the potential implications of specific extraneuronal uptake of [^{18}F]PFBG through the uptake-2 mechanism.

Key Words: catecholamine uptake; fluorine-18-PFBG; rat heart

J Nucl Med 1996; 37:2011–2016

Several scintigraphic techniques have been developed for noninvasive assessment of sympathetic neuronal function. Wieland et al. (*1–4*) reported the synthesis and use of *meta*-[^{131}I]iodobenzylguanidine (MIBG) as a single-photon imaging agent of the adrenal gland (*1*). This radiotracer also has been shown to be applicable in evaluating the sympathetic integrity of the myocardium (*5,6*) and tumors of neuroendocrine origin (*1–3,7*). MIBG has been shown to share the same uptake processes as norepinephrine (*1–4*). An advantage of MIBG is that it is resistant to neuronal enzymatic degradation by monoamine oxidase or catechol-O-methyl transferase, whereas radiolabeled norepinephrine is metabolized by these enzyme systems (*1,2*).

Mechanisms of MIBG tissue uptake that have been described include neuronal (uptake-1) and extraneuronal (uptake-2, myocyte) specific membrane transport processes and passive diffusion in and from both cellular compartments (*1,8,9*). Specific pharmacologic blockade can be used selectively to evaluate the different components of MIBG uptake in an organ such as the heart. Neuronal uptake can be blocked by the tricyclic antidepressants, with desipramine (DMI) being the most commonly used blocker (*8–11*). Chemical sympathetic denervation of the myocardium can be accomplished with 6-hydroxydopamine (*12*). Extraneuronal blockade can be effected using the chloroalkylamine SKF550 or clonidine (*8,9,13,14*). An important uptake process within the vesicles of the neuronal axon for storage of catecholamines has been discovered (*8,15*) and this process can be blocked using reserpine or Ro 4-1248.

PET radiopharmaceuticals also have been developed for the evaluation of myocardial sympathetic integrity, including [^{11}C]norepinephrine, 6-[^{18}F]fluoronorepinephrine and 6-[^{18}F]fluorometaraminol, *meta*-[^{76}Br]bromobenzylguanidine ([^{76}Br]MBBG), [^{11}C]hydroxyephedrine ([^{11}C]HED) and *para*-[^{18}F]fluorobenzylguanidine ([^{18}F]PFBG) (*16–23*). The first two compounds have not been used widely because of their rapid in vivo metabolism by intraneuronal enzyme systems (*16*). Carbon-11-HED has shown resistance to metabolism in the heart with strong myocardial neuronal retention and would be useful for repeat studies performed before and after acute cardiovascular interventions (*18,22*). However, the short physical half-life of ^{11}C ($T_{1/2}$ = 20 min) limits its use to PET centers with an in-house cyclotron.

Preliminary work using [^{18}F]PFBG in the dog has shown rapid tracer accumulation within the myocardium with prolonged myocardial retention (*24*). In dogs, [^{18}F] PFBG myocardial uptake is related in part to uptake-1, since it has been shown to be partially inhibited by DMI (*24*). Two features of [^{18}F] PFBG that make it advantageous for clinical PET studies include the longer physical half-life ($T_{1/2}$ = 109 min) relative to ^{11}C and negligible systemic metabolism (*25*).

To accurately interpret myocardial imaging studies with [^{18}F]PFBG, a better understanding of the underlying mechanisms of transport is required. The roles of the uptake-1 and uptake-2 mechanisms for the uptake and retention of [^{18}F]PFBG within the myocardium have yet to be investigated. The purpose of this study is to quantify myocardial uptake and washout kinetics of [^{18}F]PFBG in isolated rat heart. The effects of pharmacologic agents with well-defined inhibitors of benzylguanidine uptake and retention within neuronal and extraneuronal compartments of the heart were investigated. These results are compared with those from previous experiments using [^{123}I]MIBG, [^{11}C]HED and [^{76}Br]MBBG (*8,21,22*).

MATERIALS AND METHODS

The radiochemical synthesis of [^{18}F]PFBG has been reported (*23*). The final product was obtained with a 50%–55% radiochemical yield and a 95% radiochemical purity. The specific activity, determined from HPLC analysis at the end of synthesis, was greater than 3330 GBq/mmole, (900 Ci/mmole).

Received Nov. 22, 1995; revision accepted Mar. 6, 1996.
For correspondence or reprints contact: Clifford R. Berry, DVM, Department of Anatomy, Physiological Sciences and Radiology, College of Veterinary Medicine, North Carolina State University, 4700 Hillsborough St., Raleigh, NC 27606.

TABLE 1
Hemodynamic Parameters of Isolated Working Rat Hearts for Each Experimental Condition

Group no.	Inhibitor	No. of hearts	Coronary flow (ml/min/g)	Cardiac output (ml/min/g)	Heart rate (pbm)	Systolic/Diastolic pressure (mmHg)
1	Control	6	13.1 ± 3.0	25.2 ± 7.9	290 ± 62	86 ± 4/66 ± 2
2	100 n*M* DMI	6	13.7 ± 4.2	27.5 ± 7.4	265 ± 64	90 ± 4/63 ± 4
3	0.8 μM SKF550	6	13.8 ± 4.1	47.9 ± 8.5*†	295 ± 35	88 ± 2/64 ± 2
4	0.8 μM SKF550 + 100 n*M* DMI	6	13.5 ± 2.8	39.4 ± 14.0	280 ± 56	86 ± 1/65 ± 1
5	0.8 μM SKF550 + 1.0 n*M* Ro 4-1284	6	17.6 ± 2.6*	34.6 ± 3.9*‡	300 ± 38	91 ± 5/63 ± 3
6	0.8 μM SKF550 + 100 n*M* DMI chase started at 30 min	4	15.0 ± 4.4	22.0 ± 7.4‡	293 ± 45	85 ± 2/65 ± 3

Values represent mean ± s.d. for a given experimental group. Coronary flows and cardiac outputs were calculated 15 min postinitiation of [^{18}F]PFBG administration.

*Significantly different from Group 1 (all p values ≤ 0.02).

†Significantly different from Group 2 (all p values < 0.03).

‡Significantly different from Group 3 (all p values ≤ 0.02.

Isolated Rat Heart Perfusion

Animal use protocols were approved by the Institutional Animal Care and Use Committee at Duke University. Hearts were excised from pentobarbital-anesthetized, female, Sprague-Dawley rats (225–275 g). After cannulation of the aorta, retrograde perfusion of the hearts was initiated (systolic pressure = 60 mmHg), followed by cannulation of the left atrium as previously described (*8,22*). Hearts were perfused at moderate workload (preload = 7.4 mm Hg and afterload = 74 mmHg). The perfusion medium was a Krebs-Henseleit bicarbonate buffer containing 5 mM glucose and gassed with 95% O_2 and 5% CO_2. Aortic pressure was monitored using a pressure transducer that allowed recording of the systolic and diastolic pressures and heart rate. Coronary and aortic flows were measured manually and neither the coronary or aortic effluents were recirculated to the hearts. The hearts were not externally paced.

The perfusion protocol consisted of an 8-min stabilization period followed by an 8- or 10-min pulse of the perfusion medium containing [^{18}F]PFBG, followed by a 20- to 50-min washout period of just the perfusion medium. Before each perfusion, [^{18}F]PFBG was added to 350 ml of perfusion medium so that the final activity concentration was 1.5–2.0 MBq/liter [^{18}F]PFBG. Fluorine-18 radioactivity was measured using two lead-collimated 5 × 5-cm NaI(Tl) probes placed 180° apart with the heart suspended between the probes by the aortic and left atrial cannulae. The apertures of the lead collimators were 2.5 cm in diameter allowing monitoring of radioactivity over the whole heart and including a small portion of the aortic and left atrial cannulae. Coincidence detection circuitry was used to determine heart counting rates, with logging of the counts and time information on a computer.

Combinations of pharmacologic interventions were added to the perfusion medium so that blockade of the uptake-1, uptake-2, uptake-1 + uptake-2, and uptake-2 + vesicular transport processes could be effected. Six groups of experiments were made in which each group contained four to six hearts with a different set of pharmacologic blockers being added to the perfusion medium. The six experimental groups were: (Group 1) control (no additional chemicals added to the perfusate; n = 6); (Group 2) 100 n*M* of the neuronal-specific uptake inhibitor DMI (n = 6); (Group 3) 0.8 μM of the extra neuronal-specific uptake inhibitor, *N*-(9-fluorenyl)-*N*-methyl-β-chloroethylamine hydrochloride (n = 6); (Group 4) 100 n*M* DMI and 0.8 μM SKF550 (n = 6); (Group 5) SKF and 1.0 μM of the vesicular transport blocker 2-hydroxy-2-ethyl-3-isobutyl-9,10-dimethoxy-1,2,3,4,6,7-hexahydro-11(b)-H-benzo(a)quinolizine (Ro 4-1284; n = 6); and (Group 6) SKF550 block with DMI chase at 30 min (n = 4).

The apparent distribution volume (ADV (ml/g)) of myocardial [^{18}F]PFBG was computed as a function of time by normalizing the coincidence counting rate by the [^{18}F]PFBG activity concentration in the perfusate as previously described (*8,22*).

Kinetic Analysis of [^{18}F]PFBG Time-Activity Curves

The washin uptake rates and washout kinetics were calculated from the normalized myocardial time-activity curves. The uptake rate for [^{18}F]PFBG was estimated from the linear portion of the uptake curve over a 1–3.5-min interval. It was assumed that equilibrium of the [^{18}F]PFBG occurred within the first minute of delivery and that uptake thereafter reflected true uptake within the neuronal and/or extraneuronal (cellular) compartments of the heart. After switching off the [^{18}F]PFBG perfusion, a biexponential fit ($y = A_1e^{-k1x} + A_2e^{-k2x}$) was performed using a personal computer and a nonlinear, least squares regression analysis (IgorPro®, Wavemetrics, Lake Oswego, OR). Estimates of the constants A_1, k_1, A_2, k_2 were obtained for the washout of each rat heart over the entire washout period that was evaluated. For DMI and Ro 4-1284 chase experiments, the washout period was divided into an initial phase in which washout was not affected by DMI, and a late phase in which the washout of [^{18}F]PFBG was influenced by DMI. A slow turnover pool fraction was also calculated as (A_2/[A_1+A_2]). This fraction reflects the relative amount of [^{18}F] PFBG that accesses the slow turnover pool.

Statistical Analysis

The data were tabulated and expressed as mean ± s.d. A two-tail t-test for unpaired samples was used to compare the mean hemodynamic parameters, uptake rates and parameters estimated by the biexponential fit. For the DMI chase experiments, the slow clearance rate from the biexponential fit before the start (8–30 min) of the additional blockade was compared with a monoexponential washout rate after the start of the additional blockade at 30 min. A value of $p \leq 0.05$ was considered statistically significant for the hemodynamic and kinetic parameters being evaluated.

RESULTS

Hemodynamic Parameters

The mean ± s.d. data of the hemodynamic parameters are summarized in Table 1 for all experimental groups. No significant alterations were observed in heart rate and systolic and diastolic pressures. A significant increase in cardiac output was observed for each of the blocking conditions, except Group 2 (DMI) when compared with the control group (all $p \leq 0.01$). The SKF550 group had the highest cardiac output value (47.9 ±

TABLE 2
Uptake Rates and Washout Kinetics of [^{18}F]PFBG Accumulation within Isolated Working Rat Heart for Each Experimental Condition

Group no.	Inhibitor	Uptake rate (ml/min/g wet)	Percent change in uptake rate	Slow turnover pool fraction ($A_2/[A_1 + A_2]$, %)	Fast clearance half-time (min)	Slow clearance half-time (min)
1	Control	2.8 ± 0.60	NA	32 ± 6.3	5.3 ± 1.1	35.2 ± 9.7
2	100 n*M* DMI	2.2 ± 0.32	−19	7.0 ± 0.7*	4.6 ± 0.5	35.6 ± 20.5
3	0.8 μ*M* SKF550	1.2 ± 0.37*†	−58	33 ± 25	3.9 ± 3.3	31.9 ± 3.6
4	0.8 μ*M* SKF550 + 100 n*M* DMI	0.15 ± 0.02*†	−95	65 ± 8.0*†‡§‖	29.3 ± 3.4*†‡§‖	
5	0.8 μ*M* SKF550 + 1.0 μ*M* Ro 4-1284	0.77 ± 0.06*†‡	−72	2.9 ± 1.0*‡	1.6 ± 0.3*†	10.9 ± 1.4*†‡
6	0.8 μ*M* SKF550 + 100 n*M* DMI chase started at 30 min					
	Prechase	1.1 ± 0.46*†	−61	25 ± 19	2.6 ± 2.2	25.3 ± 12.6§
	Postchase	NA	NA	NA	NA	74.1 ± 17.1#

*Significantly different from Group 1 (all p values ≤ 0.001).
†Significantly different from Group 2 (all p values ≤ 0.001).
‡Significantly different from Group 3 (all p values ≤ 0.003).
§Significantly different from Group 5 (all p values ≤ 0.03).
‖Significantly different from Group 6 (all p values ≤ 0.03).
**Significantly different from prechase conditions (p value = 0.004).
Values represent mean ± s.d. for a given experimental group. NA = not applicable. Uptake rates, washout constants and $(A_2/[A_1 + A_2])$ for Group 4 were significantly different from all other groups (all p values ≤ 0.035).

8.3 ml/min/g). Coronary flow rates were significantly increased in Groups 4 and 5 ($p < 0.02$).

Uptake and Washout Kinetics

Uptake and washout parameter estimates are summarized in Table 2 for all experimental groups. Uptake-1 inhibition (Group 2) caused a 19% reduction in the uptake rate compared to control conditions (Group 1). Uptake-2 inhibition (Group 3) caused a 58% reduction in the uptake rate compared to control conditions (Group 1). Together, DMI and SKF550 (Group 5) caused a 95% decrease in [^{18}F]PFBG uptake (Fig. 1). Inhibition of vesicular transport with Ro 4-1284 caused a further 33% reduction in uptake rate when compared with the uptake rate of the SKF550 group alone (Group 3 versus Group 5, Fig. 2).

Clearance of [^{18}F]PFBG was accelerated in the DMI-blocked hearts as evidenced by a 78% decrease in the relative amplitude of the slow turnover pool fraction $(A_2/(A_1+A_2))$, Table 2. Blockade of uptake-2 by SKF550 increased the early clearance rate (k_1) by a factor of 2.6 but did not affect the later slow clearance phase. A very rapid clearance component was noted when the perfusate contained both DMI and SKF550. A small fraction (<2%) was observed to remain within the heart.

Fluorine-18-PFBG clearance from neurons was accelerated in the SKF550 perfused hearts with the addition of the vesicular blocking agent, Ro 4-1284 (Fig. 2). Decreases in the uptake rate and the slow clearance rate were observed when compared to SKF550 alone (Group 3). The k_2 values significantly increased ($p < 0.001$) from 0.022 ± 0.003 min^{-1} ($T_{1/2}$ = 32 min) in Group 3 (SKF550 alone) to 0.064 ± 0.008 min^{-1} ($T_{1/2}$ = 11 min) in Group 4 (SKF550 and Ro 4-1284). The shape of the uptake portion of the time-activity curve from Group 4 was nonlinear (Fig. 2).

Experiments were performed using SKF550 blockade and pharmacologic chasing with DMI to investigate the influence of neuronal reuptake on clearance times [^{18}F] PFBG from the heart. When DMI was given at 30 min, [^{18}F] PFBG clearance was slowed; the slow phase k_2 values significantly decreased ($p = 0.004$) from 0.032 ± 0.015 min^{-1} ($T_{1/2}$ = 22 min) to 0.007 ± 0.005 min^{-1} ($T_{1/2}$ = 99 min).

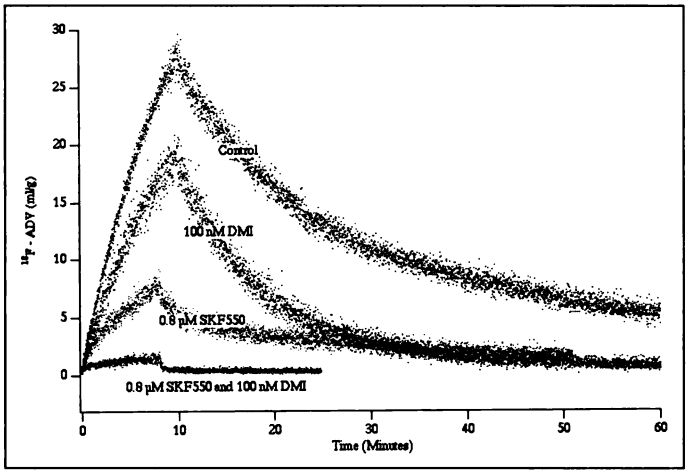

FIGURE 1. Normalized [^{18}F]PFBG uptake and retention time-activity curves are shown from representative rat hearts with and without inhibitors: DMI (uptake-1 blockade), SKF550 (uptake-2 blockade) and the combination of DMI and SKF550.

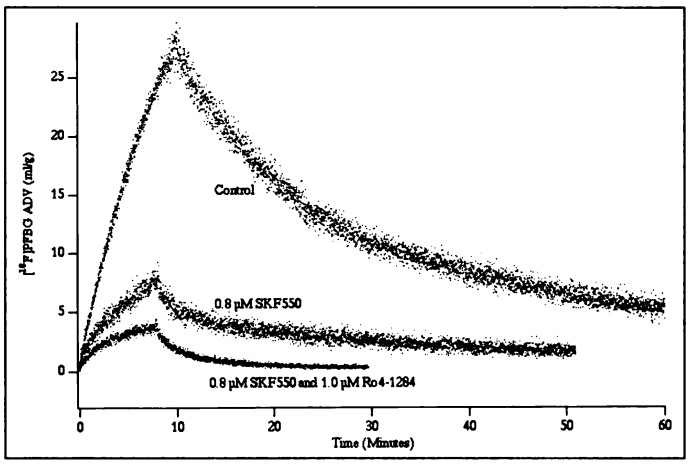

FIGURE 2. Normalized [^{18}F]PFBG time-activity curves showing a control rat heart and the effects of SKF550 (uptake-2 blockade) and the combination of SKF550 and Ro 4-1284 (uptake-2 and vesicular blockade) on myocardial kinetics of [^{18}F]PFBG.

DISCUSSION

The purpose this study was to elucidate the mechanisms of [^{18}F]PFBG uptake and clearance in the rat heart. The contributions of the uptake-1 and uptake-2 processes were evaluated using several well-defined pharmacologic interventions. The uptake-2 mechanism may be stronger in rat myocardium than in human myocardium, (*8,26,27*). Nevertheless, this experimental model enables a comprehensive characterization of potential catecholamine radiotracer analogs for both mechanisms.

Fluorine-18-PFBG is rapidly taken up by both uptake-1 into the sympathetic neurons and uptake-2 into myocytes of the isolated rat heart. Neuronal uptake of [^{18}F]PFBG is supported by vesicular sequestration of [^{18}F]PFBG and is evidenced by a reduction of the uptake rate in the uptake-2 blocked hearts with the Ro 4-1284 (Group 5 versus Group 3). The washout portion of the ADV time curves of [^{18}F]PFBG had a biexponential clearance with a rapid initial clearance (mean $T_{1/2}$ = 5.3 min) and slower delayed clearance (mean $T_{1/2}$ = 35.2 min) in control hearts. The slower clearance process may be related to binding processes within the neuron or the myocyte. Similar slow clearance rates were found in control, uptake-1 blocked and uptake-2 blocked groups (mean $T_{1/2}$ = 35.2 min, 35.6 min and 31.9 min, respectively), suggesting similar release rates from neurons and myocytes. More rapid initial washout rate was observed for the SKF550 blockade group, which is suggestive of rapid early washout from the extracellular or axoplasmic neuronal compartments.

A very rapid clearance component was seen when the perfusate contained both DMI and SKF550, likely reflecting washout of [^{18}F]PFBG from the interstitial spaces. A small fraction (<2%) was observed to remain within the heart, which is consistent with slow passive diffusion of [^{18}F]PFBG out of the neuronal and/or extraneuronal compartments.

In the uptake-2 blocked hearts, the slower clearance rate was decreased significantly by subsequent chasing with DMI. The absence of an increased clearance rate with DMI suggests that the neuronal uptake-1 mechanism is not significant for neuronal retention of [^{18}F]PFBG in isolated rat heart. On the contrary, the uptake-1 carrier may facilitate export of the axoplasmic [^{18}F]PFBG. Under conditions of high coronary flow the interstitial concentration of [^{18}F]PFBG is maintained at a low level, with evidently minimal reuptake of [^{18}F]PFBG into the neurons. Therefore, blockade of uptake-1 results in a net decreased outward flux across the neuronal membrane. A similar phenomenon was previously observed for nonexocytic release of norepinephrine from the isolated rat heart under ischemic conditions (*28*).

Cardiac output nearly doubled when SKF550 was administered in these experiments when compared with DMI blockade and control conditions. This finding was surprising since previous experiments using SKF550 did not significantly alter the cardiac output (*8*). However, in the previous experiment (*8*) only 0.4 μM SKF550 was used, whereas we used 0.8 μM SKF550 in our current study. Since we did not observe a significant difference in the heart rate and afterload, the change in cardiac output may result from an increased myocardial contractility. We do not have an explanation for this finding.

Fluorine-18-PFBG clearance from neurons was accelerated in the SKF550 perfused hearts with the addition of Ro 4-1284. Decreases in the size and rate of the slow clearance phase also were observed. These changes are consistent with a decrease in the neuronal distribution volume for [^{18}F]PFBG after vesicular transport blockade. These findings suggest that Ro 4-1284 limits [^{18}F]PFBG uptake into the vesicular spaces. When

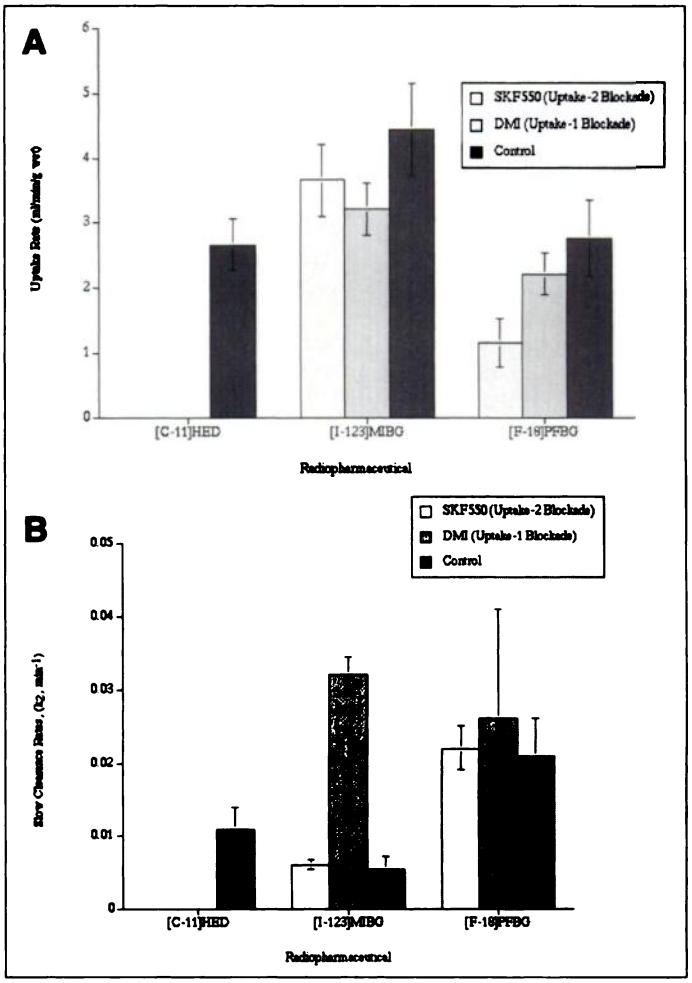

FIGURE 3. Comparison of (A) uptake rates (ml/min/g) and (B) slow clearance rates (min^{-1}) for three sympathetic neuronal radiopharmaceuticals in the isolated working rat heart: [^{11}C]HED (*22*), [^{123}I]MIBG (*8*) and [^{18}F] PFBG.

compared with the SKF550 group only (Group 3), early clearance rate (k_1) was slightly increased, while late clearance rate (k_2) was significantly greater ($p = 0.02$).

Comparison with Carbon-11-HED, Bromine-76-MBBG and Iodine-123-MIBG

A comparison of [^{18}F]PFBG with [^{11}C]HED, [^{76}Br]MBBG and [^{123}I]MIBG is of interest for physiological imaging (*8,21,22*). Similar neuronal, extraneuronal and vesicular blockade studies have been performed in the same isolated rat heart model using the various radiopharmaceuticals (Fig. 3). Direct comparison of uptake rates with [^{11}C]HED is somewhat misleading as [^{11}C]HED is known to be taken up by only an uptake-1 mechanism in the isolated rat heart and is specific to imaging only the sympathetic neuronal compartment (*22*). The uptake rate into neurons for [^{18}F]PFBG (Group 3 of this study) is about half that reported for [^{11}C]HED (control conditions), while the clearance rate of [^{18}F]PFBG is faster when compared with [^{11}C]HED. DMI blockade in the isolated rat heart resulted in nonlinear uptake of [^{11}C]HED, 83% reduction in the uptake rate of [^{11}C]HED and more rapid initial washout of [^{11}C]HED (*22*).

In chase studies where DMI was given at the time of peak [^{11}C]HED uptake, there was a 20-fold increase in the clearance rate of [^{11}C]HED (*22*), suggesting uptake-1 reuptake into neurons to be the primary retention mechanism. Carbon-11-HED uptake, however, was shown to be sensitive to elevated extracellular levels of norepinephrine, as might be seen in

patients with heart failure (*22*). DMI chase studies have shown opposite effects for [^{18}F]PFBG when compared with [^{11}C]HED; uptake-1 blockade delays the washout of [^{18}F]PFBG. These findings show [^{18}F]PFBG to have a lower velocity for uptake-1 transport relative to [^{11}C]HED. This could be advantageous because it could dissociate the uptake rate from the effects of coronary flow rates and decrease sensitivity of [^{18}F]PFBG to competitive inhibition by endogenous catecholamines in physiological imaging studies.

The utility of [^{18}F]PFBG also should be considered in relationship with other available radiohalogenated benzylguanidines such as [^{123}I]MIBG and [^{76}Br]MBBG. Compared with earlier data from studies using exchange-labeled [^{131}I]MIBG, [^{76}Br] MBBG was found to have higher neuronal specific uptake in the rat heart at 4 hr postinjection (*20,21*). However, these data must be interpreted with caution as carrier effects may have been present for the isotopic-exchange labeling of [^{131}I]MIBG, whereas [^{76}Br]MBBG is synthesized through a no-carrier added labeling procedure. Recent work by DeGrado et al. (*8*) has shown the relative volume of distribution of no-carrier added [^{123}I]MIBG in neuronal and extraneuronal compartments to be consistent with [^{76}Br]MBBG retention characteristics at 4 hr postinjection. The relative uptake percentage of [^{76}Br]MBBG within the neuron, myocyte and passive diffusion has been shown to be 63%, 12% and 25%, respectively, in the rat heart (*21*). Preliminary data with [^{76}Br]MBBG in the isolated rat heart model confirms a similar relative distribution of uptake between uptake-1 and uptake-2, although quantitative data have not been presented (*29*). Bromine-76-MBBG has been shown to have lower lipophilicity when compared with MIBG (*21*).

DeGrado et al. (*8*) have shown the relative importance of the uptake-1 and uptake-2 processes for normal uptake and retention of [^{123}I]MIBG in the isolated rat heart. A passive diffusion process was also shown to account for a small percentage of the total myocardial uptake of [^{123}I]MIBG, reflected by uptake from the interstitial space in rat hearts that were blocked with both DMI and SKF550. The use of a specific vesicular blocking chemical (Ro 4-1284) caused a more rapid clearance of the [^{123}I]MIBG, documenting the importance of intraneuronal vesicular storage of [^{123}I]MIBG as part of the neuronal retention mechanism (*8*).

There are clear differences in the transport velocities of [^{18}F]PFBG and [^{123}I]MIBG through the uptake-1 and uptake-2 transporters of the rat heart. Transport rates were 3.1 and 1.5 times higher for [^{123}I]MIBG than [^{18}F]PFBG through the uptake-1 and uptake-2 carriers, respectively (Fig. 3A). Fluorine-18-PFBG transport is relatively more efficient through the uptake-2 transporter, whereas [^{123}I]MIBG transport through both mechanisms is equally efficient. For [^{123}I]MIBG, the transport rate in control rat hearts is likely rate-limited by transcapillary transport (lower than the sum of individual uptake-1 and uptake-2 transport rates), whereas, for [^{18}F]PFBG, the overall transport rate is more closely reflective of the cellular transport rates (roughly equivalent to the sum of the uptake-1 and uptake-2 transport rates). Possible explanations of these differences might include: (a) lower lipophilicity of [^{18}F]PFBG promoting slower diffusion across the capillary barrier and/or more efficient transport through uptake-1 and uptake-2 carriers and (b) different mechanisms of intracellular binding, both within the neuronal (and vesicular) and extraneuronal space (*30*). The possibility of cellular membrane binding of the benzylguanidines has been suggested in a study by Glowniak (*30*), in which the human norepinephrine transporter protein was shown to be responsible for the neuronal binding of MIBG.

Clearance rates for [^{18}F]PFBG are faster than those previously reported for [^{123}I]MIBG, suggesting lower affinity of the fluorinated analog to intracellular binding sites or reuptake mechanisms. Neuronal clearance of [^{123}I]MIBG was discriminated from extraneuronal clearance by a fivefold lower clearance rate (*8*), whereas neuronal and extraneuronal clearance rates were similar for [^{18}F]PFBG (Fig. 3B). As with [^{123}I]MIBG, vesicular storage appears to be important for uptake and storage of [^{18}F]PFBG.

Implications for Imaging Studies

The use of [^{18}F]PFBG as a PET radiopharmaceutical for sympathetic imaging would have certain advantages over [^{123}I]MIBG based on the inherent resolution of the imaging equipment available for PET compared with SPECT. These advantages would include better spatial resolution and ability to better quantify distribution volumes of [^{18}F]PFBG due to the more accurate attenuation correction algorithms available for PET. Additionally, as the coincident detectors are located 360° around the patient, temporal resolution will be better than that possible with SPECT cameras that require rotation around the patient.

The use of [^{18}F]PFBG may have certain advantages over [^{11}C]HED for sympathetic imaging. These advantages would include: (a) good metabolic stability (*25*), (b) lower lipophilicity allowing for lower passive diffusion into the cells and a higher specificity of uptake by the carrier-mediated mechanisms, (c) practical advantage of ^{18}F ($T_{1/2}$ = 109 min) compared with ^{11}C ($T_{1/2}$ = 20 min) for clinical studies, (d) favorable neuronal clearance rates that would allow one to accurately determine the neuronal distribution volume, (e) lower flow dependence as a consequence of lower neuronal uptake rate and higher neuronal efflux, (f) higher sensitivity to vesicular function and (g) potentially lower sensitivity to competition effects with norepinephrine for uptake-1 transport, although this has yet to be evaluated. Potential disadvantages of using [^{18}F] PFBG include: (a) the strong affinity for uptake-2 as a confounding factor for those species and target organs where uptake-2 is important and (b) unknown sensitivity to changes in catecholamine metabolism and intravesicular processes.

CONCLUSION

Our results show the importance of both uptake-1 and uptake-2 mechanisms for [^{18}F]PFBG accumulation within the isolated rat heart. Neuronal uptake is supported by vesicular uptake, probably by maintenance of low levels of [^{18}F]PFBG in the axoplasm. The retention characteristics include a rapid washout phase indicative of clearance of the [^{18}F]PFBG from cellular and extracellular spaces and a slow clearance phase that, for uptake-2 blocked hearts, is nearly completely dependent on the activity of the Ro 4-1284 sensitive vesicular catecholamine transporter but not dependent on neuronal reuptake. The influence of extraneuronal disposition of [^{18}F]PFBG should be given careful consideration in PET applications using [^{18}F]PFBG for imaging the myocardium, particularly in animal species known to have a significant uptake-2 mechanism for catecholamine uptake. Indication of neuronal processing of [^{18}F]PFBG may be possible in species with negligible inherent uptake-2 activity or with specific pharmacologic blockade of the extraneuronal uptake mechanism.

ACKNOWLEDGMENTS

This work was supported by Department of Energy grant DE-FG02-96ER62148 and the State of North Carolina. We thank the companies SmithKline-Beecham and Hoffmann-La. Roche for their provision of the chemicals. Portions of this work were previously presented at the Ninth International Symposium on Radiopharmacology, 1995, and the Annual Meeting of the American College of Veterinary Radiology,1995. A preliminary report of our work has been reported and published (*31*).

REFERENCES

1. Wieland DM, Swanson DP, Brown EL, Beierwaltes WH. Imaging, the adrenal medulla with an ^{131}I-labeled antiadrenergic agent. *J Nucl Med* 1979;20:155–158.
2. Wieland DM, Wu JL, Brown LE, et al. Radiolabeled adrenergic neuron-blocking agents: adrenomedullary imaging with [^{131}I]iodobenzylguanidine. *J Nucl Med* 1980; 21:349–353.
3. Wieland DM, Mangner TJ, Inbasekaran MN, et al. Adrenal medulla imaging agents: a structure-distribution relationship study of radiolabeled aralkylguanidines. *J Med Chem* 1984;27:149–155.
4. Wieland DM, Brown LE, Rogers WL, et al. Myocardial imaging with a radioiodinated norepinephrine storage analog. *J Nucl Med* 1981;22:22–31.
5. Glowniak JV, Turner FE, Gray LL, et al. Iodine-123 metaiodobenzylguanidine imaging of the heart in idiopathic congestive cardiomyopathy and cardiac transplants. *J Nucl Med* 1989;30:1182–1191.
6. Merlot P, Valette H, Dubois-Randê, et al. Prognostic value of cardiac metaiodobenzylguanidine imaging in patients with heart failure. *J Nucl Med* 1992;33:471–477.
7. Hanson MW, Feldman JM, Beam CA, et al. Iodine-131-labeled metaiodobenzylguanidine scintigraphy and biochemical analysis in suspected pheochromocytoma. *Arch Interr Med* 1991;151:1397–1402.
8. DeGrado TR, Zalutsky MR, Vaidyanathan G. Uptake mechanisms of meta-[^{123}I]iodobenzylguanidine in isolated rat heart. *Nucl Med Biol* 1995;22:1–12.
9. Trendelenburg U. Extraneuronal uptake and metabolism of catecholamines as a site of loss. *Life Sci* 1978;22:1217–1222.
10. Iversen LL, Salt PJ, Wilson HA. Inhibition of catecholamine uptake in the isolated rat heart by haloalkylamines related to phenoxybenzamine. *Br J Pharmacol* 1972;46:647–657.
11. Tobes MC, Jaques S, Wieland DM, Sisson JC. Effect of uptake-1 inhibitors on the uptake of norepinephrine and metaiodobenzylguanidine. *J Nucl Med* 1985;26:897–907.
12. Dae MW, DeMarco T, Botvinick EH, et al. Scintigraphic assessment of MIBG uptake in globally denervated human and canine hearts–implications for clinical studies. *J Nucl Med* 1992;33:1444–1450.
13. Lightman SL, Iversen LL. The role of uptake$_2$ in the extraneuronal metabolism of catecholamines in the isolated rat heart. *Br J Pharmacol* 1969;37:638–649.
14. Salt PJ. Inhibition of noradrenaline uptake-2 in the isolated rat heart by steroids, clonidine and methoxylated phenylethylamine. *Eur J Pharmacol* 1972;20:329–340.
15. Nakajo M, Shimabukuro K, Yoshimura H, et al. Iodine-131 metaiodobenzylguanidine intra- and extravesicular accumulation in the rat heart. *J Nucl Med* 1986;27:84–89.
16. Ding Y-S, Fowler JS, Dewey SL, et al. Comparison of high specific activity (+)- and (-)-6-[^{18}F]fluoronorepinephrine and 6-[^{18}F]fluorodopamine in baboons: heart uptake, metabolism and the effect of desipramine. *J Nucl Med* 1993;34:619–629.
17. Wieland DM, Rosenspire KC, Hutchins GD. Neuronal mapping of the heart with 6-[^{18}F]fluorometaraminol. *J Med Chem* 1990;33:956.
18. Schwaiger M, Kalff V, Rosenspire KC, et al. Noninvasive evaluation of sympathetic nervous system in human heart by PET. *Circulation* 1993;82:457–464.
19. Schwaiger M, Guibourg H, Rosenspire KC, et al. Effect of regional myocardial ischemia on sympathetic nervous system as assessed by ^{18}F-metaraminol. *J Nucl Med* 1990;31:1352–1357.
20. Valette H, Loc'h C, Mardon K, et al. Bromine-76-metabromobenzylguanidine: a PET radiotracer for mapping sympathetic nerves of the heart. *J Nucl Med* 1993;34:1739–1744.
21. Loc'h C, Mardon K, Valette H, et al. Preparation and pharmacological characterization of [^{76}Br]-*meta*-Bromobenzylguanidine ([^{76}Br]MBBG). *Nucl Med Biol* 1994;21:49–55.
22. Degrado TR, Hutchins GD, Toorongian SA, et al. Myocardial kinetics of ^{11}C-*meta*-hydroxyephedrine retention mechnanisms and effects of norepinephrine. *J Nucl Med* 1993;34:1287–1293.
23. Garg PK, Garg S, Zalutsky MR. Synthesis and preliminary evaluation of *para*- and *meta*-[F-18]fluorobenzylguanidine. *Nucl Med Biol* 1994;21:97–103.
24. Garg PK, Berry CR, DeGrado TR, et al. Myocardial and adrenal uptake of *para*-[^{18}F]fluorobenzylguanidine in the dog [Abstract]. *J Nucl Med* 1994;35:255P.
25. DeGrado TR, Garg PK, Berry CR, et al. Compartmental model estimation and parametric imaging of distribution volume of sympathetic neuronal tracer *para*-[^{18}F-]fluorobenzylguanidine (PFBG) in canine myocardium [Abstract]. *J Nucl Med* 1995; 36(suppl):38P.
26. Carr EA, Carroll M, Counsell RE, Tyson JW. Studies of uptake of the bretylium analog, iodobenzyltrimethylammonium iodid, by nonprimate, monkey and human hearts. *Br J Pharmacol* 1979;8:425–432.
27. Esler M, Jackman G, Leonard P, et al. Effect of norepinephrine uptake blockers on norepinephrine kinetics. *Clin Pharmacol Ther* 1981;29:12–20.
28. Schömig A. Catecholamines in myocardial ischemia: systemic and cardiac release. *Circulation* 1990;82(suppl II):II-13–II-22.
29. Raffel D, Loc'h C, Mardon K, et al. Kinetics of ^{76}Br metabromobenzylguanidine (MBBG) in isolated rat heart: estimation of Michaelis-Menten constants for uptake-1 and uptake-2 [Abstract]. *J Nucl Med* 1994;35(suppl):57P.
30. Glowniak JV, Kitty JE, Amara SG, et al. Evaluation of metaiodobenzylguanidine uptake by the norepinephrine, dopamine and seratonin transporters. *J Nucl Med* 1993;34:1140–1146.
31. DeGrado TR, Berry CR, Garg PK, et al. Uptake and retention mechanisms of *para*-[^{18}F] fluorobenzylguanidine (PFBG) in rat heart [Abstract]. *Q J Nucl Med* 1995;39:22–24.